

In Vitro Activities of Hexaazatrinaphthylenes against *Leishmania* spp.

Atteneri López-Arencibia,^a Daniel García-Velázquez,^b Carmen M. Martín-Navarro,^a Ines Sifaoui,^c María Reyes-Batlle,^a Jacob Lorenzo-Morales,^a Ángel Gutiérrez-Ravelo,^b José E. Piñero^a

University Institute of Tropical Diseases and Public Health of the Canary Islands, University of La Laguna, Tenerife, Canary Islands, Spain^a; Instituto Universitario de Bio-Organica Antonio González, Departamento de Química Orgánica, Universidad de La Laguna, Tenerife, Spain^b; Laboratoire Matériaux-Molécules et Applications, IPEST, University of Carthage, La Marsa, Tunisia^c

The *in vitro* activity of a novel group of compounds, hexaazatrinaphthylene derivatives, against two species of *Leishmania* is described in this study. These compounds showed a significant dose-dependent inhibition effect on the proliferation of the parasites, with 50% inhibitory concentrations (IC₅₀s) ranging from 1.23 to 25.05 μ M against the promastigote stage and 0.5 to 0.7 μ M against intracellular amastigotes. Also, a cytotoxicity assay was carried out in order to evaluate the possible toxic effects of these compounds. Moreover, different assays were performed to determine the type of cell death induced after incubation with these compounds. The obtained results highlight the potential use of hexaazatrinaphthylene derivatives against *Leishmania* species, and further studies should be undertaken to establish them as novel leishmanicidal therapeutic agents.

Leishmania species are obligate intracellular parasites that are transmitted to the mammalian host by the bites of infected sand flies. Cutaneous leishmaniasis (CL), the most common form, is a group of diseases with a spectrum of clinical manifestations, ranging from small cutaneous nodules to widespread mucosal tissue destruction (1). Visceral leishmaniasis (VL) is the most severe form, as the parasites migrate to vital organs. It is a severe, debilitating disease, characterized by prolonged fever, splenomegaly, hypergammaglobulinemia, and pancytopenia. Patients gradually become ill over a period of a few months, and the disease is often fatal if left untreated (2).

The World Health Organization (WHO) estimates that 1.5 million cases of CL and 500,000 cases of VL occur every year in 82 countries. CL is endemic in more than 70 countries worldwide, and 90% of the cases occur in Afghanistan, Algeria, Brazil, Pakistan, Peru, Saudi Arabia, and Syria (3, 4). VL is presented in 65 countries; the majority (90%) of cases occur in agricultural areas and among the suburban depressed areas of five countries, Bangladesh, India, Nepal, Sudan, and Brazil (5). Estimates indicate that there are approximately 350 million people at risk for acquiring leishmaniasis, with 12 million currently infected worldwide (6).

The current available leishmanicidal treatments include pentavalent antimonials, amphotericin B, miltefosine, paromomycin, and pentamidine (7). These drugs can be administered alone or in combination (8, 9, 10). However, combinations of these drugs are normally highly toxic to the patient even at low doses. Furthermore, most of these treatments require several days of hospitalization because of the use of intravenous or parenteral administration of the drug. These side effects include teratogenic effects, nephrotoxicity, pancreatitis, ototoxicity, and fever, among others. Nevertheless, the appearance of strains resistant to these active compounds presents a major problem in the current therapeutic measures against these parasites (11, 12). Moreover, since there is no immediate prospect of efficacious vaccines on the horizon (13), there is a great need to develop novel leishmanicidal agents with an acceptable efficacy and safety profile.

Derivatives of 5,6,11,12,17,18-hexaazatrinaphthylene (5,6,11,12,17,18-HATN; diquinoxalino [3,3-a:2',3'-c] phenazine) have recently attracted attention as materials for organic electronic applications. These compounds can, depending on the choice of substituent, form films with a wide range of morphologies, in-

cluding organogels and columnar discotic liquid-crystalline and amorphous solids (14, 15, 16).

No data are available that represent the activity of these products against any pathogen; however, it has been reported that 1,2,4,5-benzenetetraamine tetrahydrochloride (DGV-B), also known as Y15, which is precursor of hexaazatrinaphthylene synthesis, has been recently used as an anticancer drug. Y15 has been shown to be able to decrease the growth rates of some tumors, such as those of breast cancer, human pancreatic tumor, human neuroblastoma, colon cancer, and thyroid cancer, by inhibiting the focal adhesion kinase (FAK), even *in vivo* (17, 18, 19, 20, 21, 22). This small molecule inhibits cellular viability in breast cancer cells at doses of 10 μ M (17) and human neuroblastoma cells in a range of 10 to 25 μ M (19).

In this study, the *in vitro* activity of various hexaazatrinaphthylene derivatives as well as their effects at the cellular death level were evaluated against two species of *Leishmania*. The obtained results highlight a potential use of these active compounds for the treatment of leishmaniasis in the near future.

MATERIALS AND METHODS

Chemicals. Members of a family of water-soluble π -conjugated hexaazatrinaphthylenes (HATNs), named DGV-A, DGV-C, and DGV-D, were synthesized in this study (Fig. 1). The synthesis of these molecules was based on the condensation of hexaketocyclohexane octahydrate and 1,2,4,5-benzenetetraamine tetrahydrochloride (DGV-B) building blocks using a short and efficient microwave-assisted reaction. The DGV-B compound was purchased from Sigma-Aldrich (Madrid, Spain). Compounds DGV-A and DGV-D were synthesized as previously described (16). DGV-C was synthesized ac-

Received 28 January 2015 Returned for modification 10 February 2015

Accepted 1 March 2015

Accepted manuscript posted online 9 March 2015

Citation López-Arencibia A, García-Velázquez D, Martín-Navarro CM, Sifaoui I, Reyes-Batlle M, Lorenzo-Morales J, Gutiérrez-Ravelo A, Piñero JE. 2015. *In vitro* activities of hexaazatrinaphthylenes against *Leishmania* spp. *Antimicrob Agents Chemother* 59:2867–2874. doi:10.1128/AAC.00226-15.

Address correspondence to Atteneri López-Arencibia, atlopez@ull.edu.es.

Copyright © 2015, American Society for Microbiology. All Rights Reserved.

doi:10.1128/AAC.00226-15

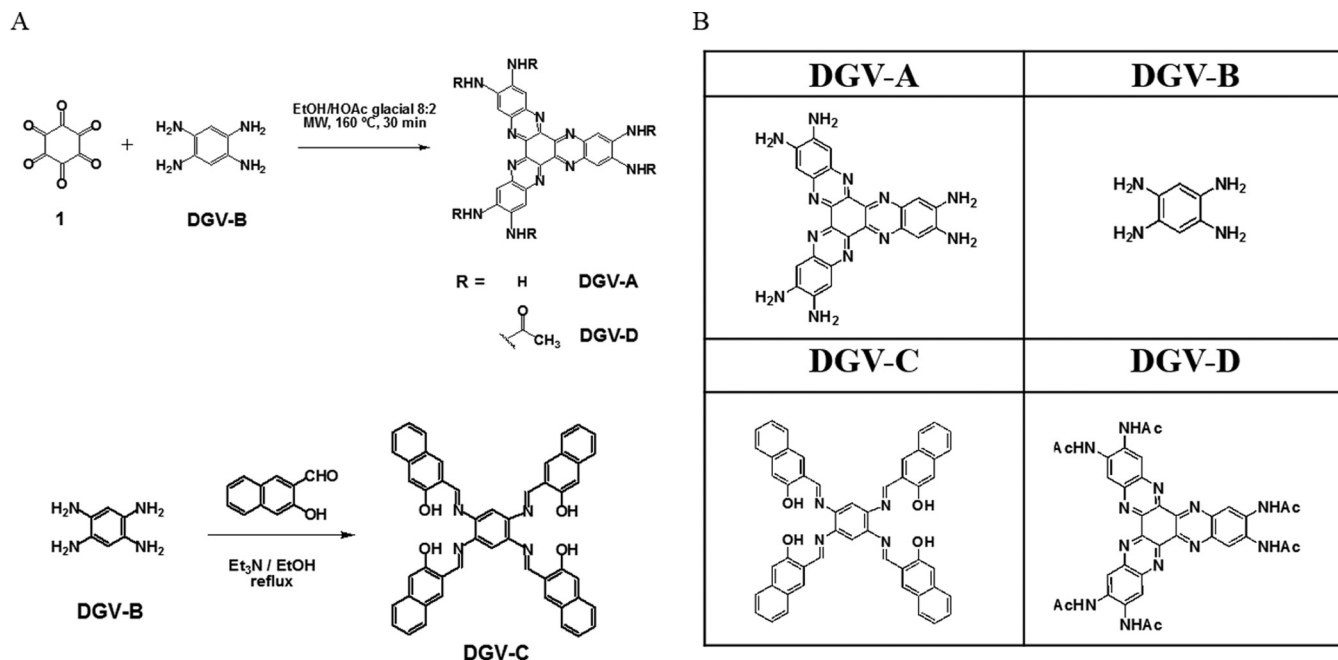


FIG 1 Synthesis (A) and structures (B) of the evaluated hexaazatrinaphthylenes. MW, microwaves.

according to the following procedure: an EtOH solution (5 ml) of 2-hydroxy-1-naphthaldehyde (0.07 g, 0.42 mM) was added dropwise to a hot EtOH solution (1 ml) of DGV-B (0.03 g, 0.1 mM). The mixture was stirred at reflux for 12 h and was cooled at -10°C , and the resulting precipitate was filtered, washed with cold EtOH, and dried under a vacuum to give DGV-C (0.061 g, 0.08 mM) as a yellow solid with an 80% yield (Fig. 1). Synthesis and characterization of the DGV-A, DGV-C, and DGV-D products were carried out in a previous study (23). All molecules were analyzed by ^1H nuclear magnetic resonance (^1H -NMR) and ^{13}C -NMR, UV/visible-light spectra, matrix-assisted laser desorption ionization–time of flight mass spectrometry (MALDI-TOF MS), and elemental analysis.

Parasite cultures. Experiments were carried out with *Leishmania amazonensis* (MHOM/BR/77/LTB0016) and *Leishmania donovani* (MHOM/IN/90/GE1F8R) strains. Promastigotes of both strains were cultured in Schneider's medium (Sigma-Aldrich, Madrid, Spain) supplemented with 10% fetal bovine serum at 26°C and were grown to the log phase per previous methods for use in further experiments. For some of the assays, the parasites were also cultured in RPMI 1640 medium (Gibco), with or without phenol red.

The J774A.1 (ATCC TIB-67) murine macrophage cell line was cultured in RPMI 1640 medium supplemented with 10% fetal bovine serum at 37°C in a 5% CO_2 atmosphere.

Activity assays for the promastigote stage of *Leishmania* spp. The activity of the HATNs was tested *in vitro* using the promastigote stage of *L. amazonensis* and *L. donovani* and a colorimetric assay based on alamarBlue reagent (Invitrogen/Life Technologies, Madrid, Spain) as previously described (24).

Briefly, hexaazatrinaphthylenes were serially diluted in 100 μl RPMI 1640 medium (Gibco/Life Technologies, Madrid, Spain) without phenol red and supplemented with 10% heat-inactivated fetal bovine serum in 96-well plates. After that, parasites in the log phase of growth were counted and diluted ($10^5/\text{well}$) and were also added to these wells. Finally, 10% alamarBlue was added to the plates, and these were incubated at 27°C . After 72 h, the plates were analyzed using an EnSpire multimode plate reader (PerkinElmer, Madrid, Spain), a test wavelength of 570 nm, and a reference wavelength of 630 nm. Percentages of inhibition and 50% inhibitory concentrations (IC_{50} s) were calculated by no-linear-regression analysis with 95% confidence limits

using Sigma Plot 12.0 statistical analysis software (Systat Software). All experiments were performed three times each in duplicate, and the mean values were also calculated. A paired two-tailed *t* test was used for analysis of the data. Values of *P* of <0.05 were considered significant.

Activity assays against intracellular amastigotes. Macrophages were plated in 96-well plates (2.5×10^5 cells/ml), infected with metacyclic stage promastigotes (~ 5 -to-6-day-old culture) of *L. amazonensis* in a 1:20 ratio, and incubated overnight for internalization. After removal of noninternalized promastigotes by extensive washing with RPMI 1640 medium, parasitized cells were incubated with medium (untreated control) or with a range of concentrations of HATNs as described above for the promastigote stage assays and incubated for 24 h at 37°C and 5% CO_2 . For the parasite rescue, controlled lysis of *L. amazonensis* amastigote-infected macrophages was performed as previously described with minor modifications (25). Briefly, the 96-well plate was washed with serum-free RPMI 1640 culture medium, and then the medium was removed and 20 μl of RPMI 1640 (with 0.05% SDS) was added to each well. After that, the plate was shaken for 30 s and 180 μl of RPMI 1640 (with 10% FBS) was added to each well. Finally, 10 μl of alamarBlue was added into each well of the 96-well plates and the mixture was incubated at 26°C . The plates were incubated at 26°C for transformation of rescued amastigotes to promastigotes. After 72 h, the plates were analyzed using an EnSpire multimode plate reader (PerkinElmer, Madrid, Spain) with an excitation wavelength of 570 nm and an emission wavelength of 585 nm. Percentages of inhibition and 50% inhibitory concentrations (IC_{50}) were calculated as previously described using Sigma Plot 12.0 statistical analysis software. All experiments were performed three times each in duplicate, and the mean values were also calculated.

Cytotoxicity assay. A commercial kit was used for the evaluation of drug-induced cytotoxic effects based on the measurement of lactate dehydrogenase (LDH) activity released to the media (LDH cytotoxicity detection kit; Roche Applied Science, Madrid, Spain), following the manufacturer's instructions. Briefly, the macrophages were incubated with different concentrations of the HATNs for 24 h in duplicate. After incubation, supernatants were obtained and LDH levels were determined following the manufacturer's instructions. To determine the cytotoxicity percentages, the average absorbance values of the duplicates were calculated and compared

with those calculated for the negative and positive controls. Cytotoxicity levels were determined as previously described (26).

Changes in the mitochondrial membrane potential ($\Delta\Psi_m$). The $\Delta\Psi_m$ was measured using a JC-1 mitochondrial membrane potential assay kit (Cayman Chemical, Vitro, Madrid, Spain) as previously described (27). Briefly, this lipophilic cationic probe accumulates in the mitochondrial matrix according to the membrane potential. In healthy cells with a high $\Delta\Psi_m$, JC-1 spontaneously forms complexes known as J-aggregates, showing intense red fluorescence (emission at 595 nm). In apoptotic or unhealthy cells with a low $\Delta\Psi_m$, JC-1 remains in its monomeric cytosolic form and shows only green fluorescence (emission at 535 nm). In brief, the promastigotes, after 24 h with different concentrations of HATNs, were harvested and washed with buffer. The cells were then incubated at 26°C for 30 min with JC-1 dye. Cells were then analyzed by fluorescence measurement in black plates through the use of a spectrofluorometer and 490 nm as the excitation wavelength. Data presented here are representative of the results of three experiments. The ratio of the reading at 595 nm to the reading at 535 nm was considered the relative $\Delta\Psi_m$ value.

Analysis of ATP levels. ATP levels were measured using a Cell Titer-Glo luminescent cell viability assay (Promega), which generates a signal proportional to the ATP amount. Promastigotes were incubated with different concentrations of HATNs for 24 h. Aliquots were taken and mixed with the kit reagent into white plates following the manufacturer's instructions for posterior measurement of the luminescence on a Perkin-Elmer spectrophotometer.

Phosphatidylserine externalization. An annexin V/propidium iodide (PI) double-staining assay was performed using a Tali apoptosis kit, annexin V, Alexa Fluor 488, and propidium iodide according to the manufacturer's instructions (Life Technologies). Briefly, after being treated with the IC₅₀ and IC₉₀ of the tested molecules for 24 h, promastigotes were centrifuged at 1,500 rpm for 10 min, washed twice with the annexin binding buffer (ABB), and incubated with 5 μ l of annexin V for 20 min. After that, cells were centrifuged and resuspended in ABB containing 1 μ l of PI and incubated for 3 min at room temperature. Finally, a 25- μ l volume of the stained cells was loaded into a Tali cellular analysis slide and was analyzed in a Tali image-based cytometer. Data were collected using Tali data acquisition and analysis software (Life Technologies Corporation).

Plasma membrane permeability. The Sytox Green assay was performed to detect alterations in membrane permeability for the parasites. Briefly, 2×10^7 promastigotes/ml were incubated with Sytox Green at a final concentration of 1 μ M (Molecular Probes) for 30 min in the dark at 26°C. Subsequently, parasites were moved to black plates and the tested compounds were added at the IC₅₀ and IC₉₀. The increase in fluorescence due to binding of the fluorescent marker to the parasitic DNA was measured using an EnSpire multimode plate reader (PerkinElmer, Madrid, Spain) with an excitation wavelength of 504 nm and an emission wavelength at 523 nm and was expressed as the percentage relative to the amount measured for fully permeabilized cells achieved by the addition of 0.1% Triton X-100 (28).

TUNEL assay. A terminal deoxynucleotidyltransferase-mediated dUTP-biotin nick end labeling (TUNEL) universal apoptosis detection kit (Genscript) was used to detect fragmented DNA by enzymatic labeling of DNA strand breaks with biotin-dNTP and terminal deoxynucleotidyl transferase (TdT). Briefly, slides with 1×10^6 cells were fixed in 4% paraformaldehyde (pH 7.4) for 1 h at room temperature, washed with phosphate-buffered saline (PBS), and incubated for 10 min with 3% H₂O₂-methanol to block nonspecific peroxidase activity. Cells were washed again with PBS and then suspended in permeabilization solution (0.1% Triton X-100–0.1% sodium citrate) for 2 min on ice. Cells were washed again, resuspended in a 50- μ l TUNEL reaction mixture or in a 50- μ l label solution alone (negative control) for 60 min, and incubated in a humidified dark chamber at 37°C, followed by washing with PBS. Cells were then resuspended in a 50- μ l streptavidin-horseradish peroxidase (HRP) solution. Peroxidase activity was revealed with DAB (3,3'-diaminobenzidine) substrate (Chromogen), and slides were analyzed using visible-light microscopy.

DNA condensation. For the detection of condensed chromatin, a double-stain apoptosis detection kit (Hoechst 33342-PI) was utilized. Parasites were treated with the HATNs (IC₅₀ and IC₉₀) for 24 h and then harvested and centrifuged. The cell pellet was resuspended in buffer with Hoechst 33342 and incubated in darkness for 15 min at 27°C. Next, propidium iodide was added in darkness for an additional 15 min at 37°C. A fluorescence microscope (Leica TCS; Leica Microsystems) was used to observe the cells, using an excitation wavelength of 588 nm and emission wavelengths of 460 nm (Hoechst) and 575 nm (PI).

RESULTS AND DISCUSSION

The incubation of the parasites with the four compounds resulted in a dose-dependent inhibition effect on the proliferation of the two tested *Leishmania* strains. The data determined for the promastigote stage (Table 1) showed very low values of IC₅₀. Furthermore, DGV-C presented IC₅₀s of 1.2 and 4.7 μ M for the promastigote stages of *L. amazonensis* and *L. donovani*, respectively. Moreover, DGV-B showed an IC₅₀ of 2.4 μ M for *L. amazonensis* and DGV-A and an IC₅₀ of 1.5 μ M for *L. donovani* promastigotes. In contrast, DGV-D presented the lowest IC₅₀ values, 13.5 and 10.2 μ M, for the promastigotes of *L. amazonensis* and *L. donovani*, respectively. In addition, the activities against the intracellular amastigotes of *L. amazonensis* were higher (Table 1), with IC₅₀s of 0.54 μ M for DGV-B and 0.71 μ M for DGV-C. However, products DGV-A and DGV-D did not show any activity against the amastigote stage of the tested *Leishmania* spp. Therefore, the rest of the assays were carried out with only the DGV-B and DGV-C compounds.

The toxicity values (calculated 50% cytotoxicity [CC₅₀] [Table 1]) of these compounds tested against murine macrophages were 46.1 and 17.5 μ M for DGV-B and DGV-C, respectively.

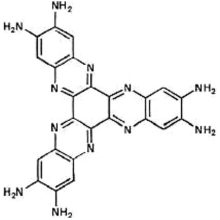
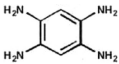
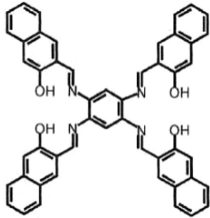
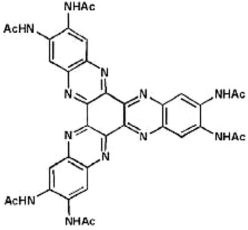
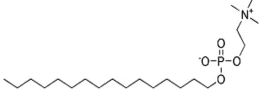
The selectivity index (SI) was also calculated, revealing that the SI for parasites of DGV-B was 86, which was higher than the value calculated for DGV-C, with an SI of 25. The index was calculated using the IC₅₀ for the intracellular stage of the parasite and the calculated CC₅₀. While some molecules used in therapy present an SI higher than 1,000, other cytotoxic products generally present SI values lower than 10 (29).

The results for the mitochondrial membrane potential ($\Delta\Psi_m$), expressed as the ratio of the data calculated at 595 nm to those calculated at 535 nm, indicate the polarization grade of the mitochondria in a cell culture (Fig. 2). In our study, both molecules induced a decrease in the mitochondrial membrane potential in both parasitic strains. This observed membrane potential decrease was higher in the case of *L. amazonensis*, where the differences between the negative control and the treated cells were statistically very significant, reducing the membrane potential to 50% of that of the control. In *L. donovani*, the reduction of the membrane potential was lower at around 25% of the control level.

The result seen with the negative control (parasites without treatment) was considered to represent 100% of the ATP level. This assay proved a potent effect of DGV-B in decreasing the ATP levels in just 24 h after treatment in both strains (Fig. 2), reaching 10% compared to the control in *L. amazonensis* and 25% in *L. donovani*. DGV-C did not show any effect on the ATP levels of *L. amazonensis* parasites, although it did decrease the ATP levels in *L. donovani* to 80%.

In live cells, phosphatidylserine (PS) is located on the cytoplasmic surface of the cell membrane. In apoptotic cells, however, PS is translocated from the inner surface to the outer surface of the plasma membrane, exposing it to the extracellular environment. The human anticoagulant annexin V displays high affinity for PS.

TABLE 1 Activity and cytotoxicity of the tested HATNs

Molecular structure	Drug	IC ₅₀ ± SD (μM)			SI	J774A.1 CC ₅₀ (μM)
		<i>L. amazonensis</i> promastigote	<i>L. donovani</i>	<i>L. amazonensis</i> amastigote		
	DGV-A	11.57 ± 1.83	1.47 ± 0.14	w/a ^a		>100
	DGV-B	2.36 ± 0.28	25.05 ± 0.01	0.536 ± 0.135	86.1	46.13
	DGV-C	1.23 ± 0.09	4.66 ± 0.98	0.709 ± 0.455	24.7	17.53
	DGV-D	13.52 ± 1.35	10.23 ± 0.11	w/a		68.14
	Miltefosine	6.48 ± 0.24	3.32 ± 0.27	3.12 ± 0.30	23.2	72.19

^a w/a, without activity.

After a cell population is stained, using a Tali apoptosis assay kit, apoptotic cells display green fluorescence, dead cells display red and green fluorescence, and live cells show little or no fluorescence. Figure 3 represents all the percentages obtained after analysis of the results in this study.

In *L. amazonensis*, stained in green with the annexin V, a strong increment of the cellular phosphatidylserine externalization was observed, reaching 70% in the case of DGV-B treatment compared to the 13% observed in the control. These data indicate the presence of an apoptosis-like process, with a strong increase of the apoptotic population in the cell culture. On the other hand, the percentage of dead cells in the population stained in red with propidium iodide (only 9% in the control) remained stable.

In the case of *L. donovani*, after 48 h of treatment, an increment of PS externalization was also observed. Moreover, it was higher in cells treated with DGV-B (36%) than in cells treated with DGV-C (7%) and the control (1%). There was also an increase (between 20% and 30%) in the proportion of dead cells seen when the

culture was incubated with these molecules compared with the observed 3% of dead cells in the control.

The assays were carried out during different hours of treatment; however, 48 h was selected as the optimal time to observe the apoptotic population. Parasites were not able to show any fluorescence (live cells only) at 24 h, and the majority of the cells on the treated culture were stained in red (dead) at 72 h.

Both *Leishmania* species were treated at the promastigote stage with Sytox Green for the study of the plasma membrane permeability, and fluorescence was measured until signal stabilization was reached. After that, the drugs were added and the fluorescence was measured during 6 h to observe the possible changes in the parasite membrane permeability. Amphotericin B (10 μM) was used as a positive control. In the case of the HATNs, the previously calculated IC₉₀ was used in this experiment. At the end of the sixth hour, Triton X-100 was added into each well in order, and the results were calculated to represent the percentage relative to Triton X-100 (100% permeabilized cells) (Fig. 4). While amphoteri-

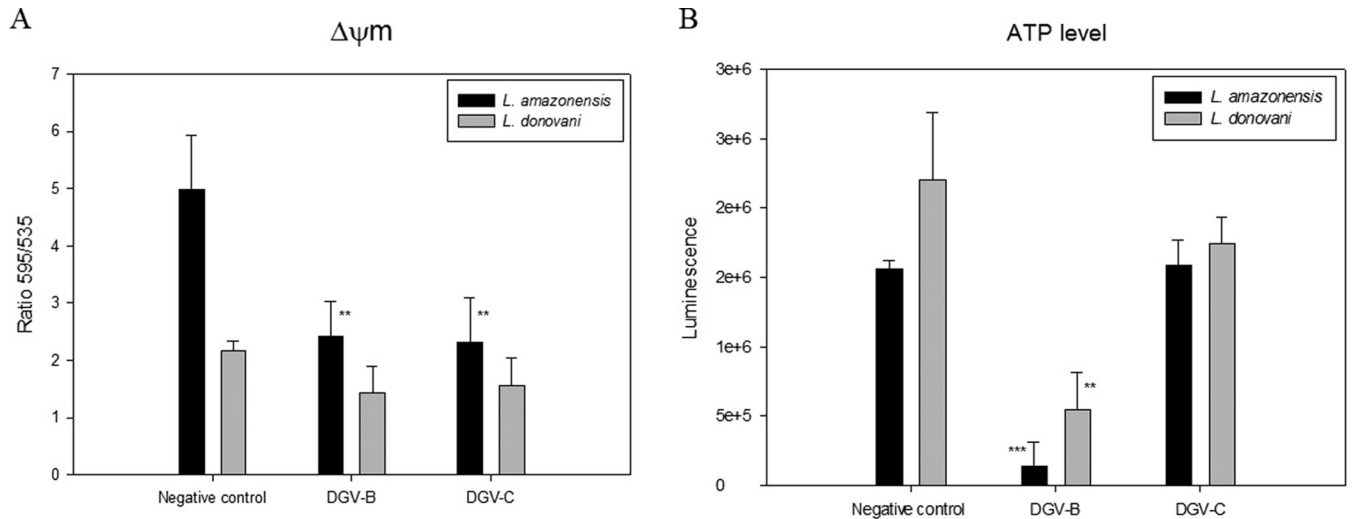


FIG 2 (A) Changes in the mitochondrial membrane potential ($\Delta\Psi_m$) of *L. amazonensis* and *L. donovani* after 24 h of incubation with the IC_{90} of DGV-B and DGV-C. (B) ATP levels of *L. amazonensis* and *L. donovani* after 24 h of incubation with the IC_{90} of DGV-B and DGV-C. Error bars represent the standard deviations (SD). Each data point indicates the mean of the results of three measurements.

cin B induced a strong increment of the permeability in both strains after 1 to 2 h, the negative control and the cells treated with either of two HATNs did not show any change, remaining stable for 6 h. Results confirmed that the plasma membrane integrity was

not altered in the parasites treated with the studied molecules, at least in the first 6 h of treatment.

The TUNEL assay revealed dark brown precipitates in the nucleus in the case of *L. donovani* promastigotes treated with DGV-B

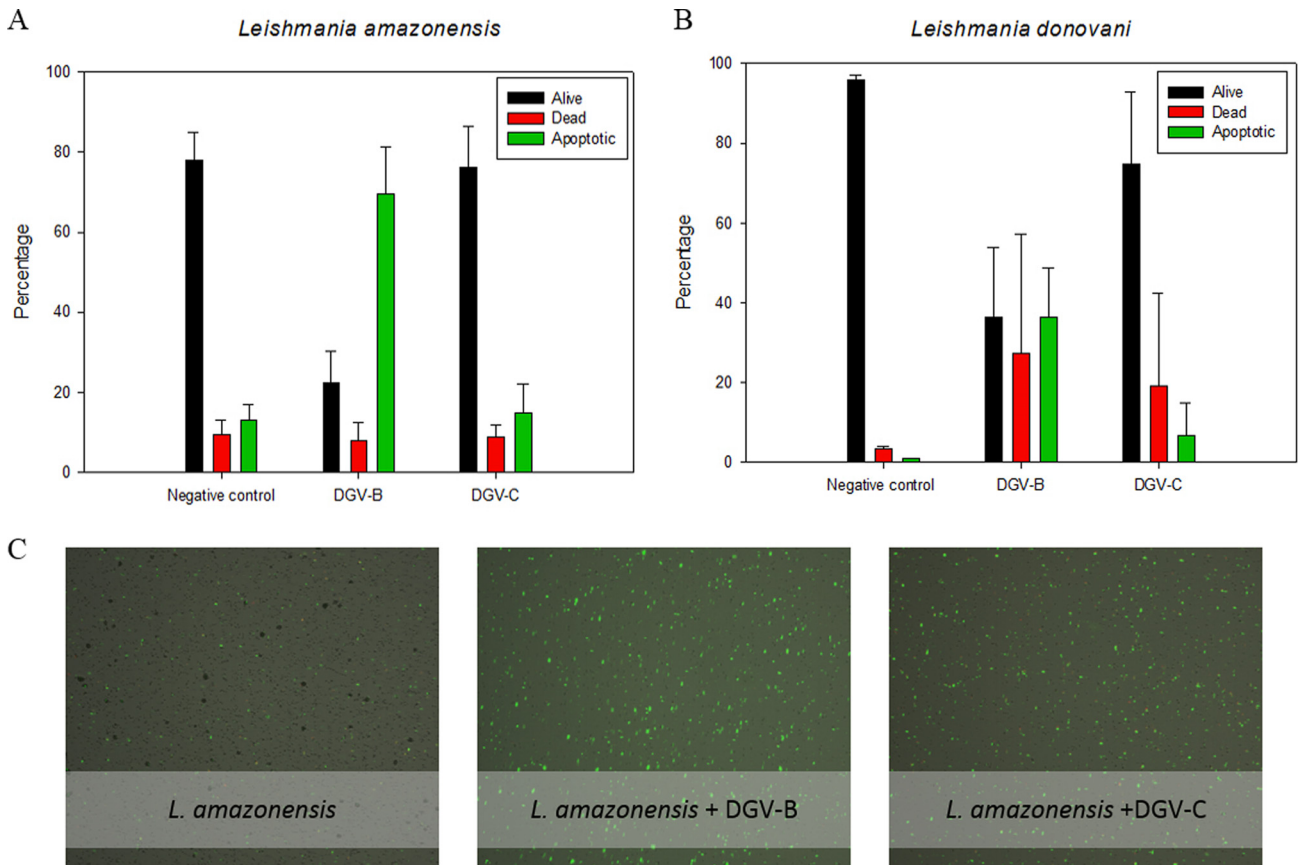


FIG 3 Results of the phosphatidylserine exposure after 48 h of incubation with the IC_{90} of DGV-B and DGV-C. (A) *L. amazonensis*. (B) *L. donovani*. (C) Images were captured using a Tali image-based cytometer. Error bars represent the standard deviations (SD). Each data point indicates the mean of the results of three measurements.

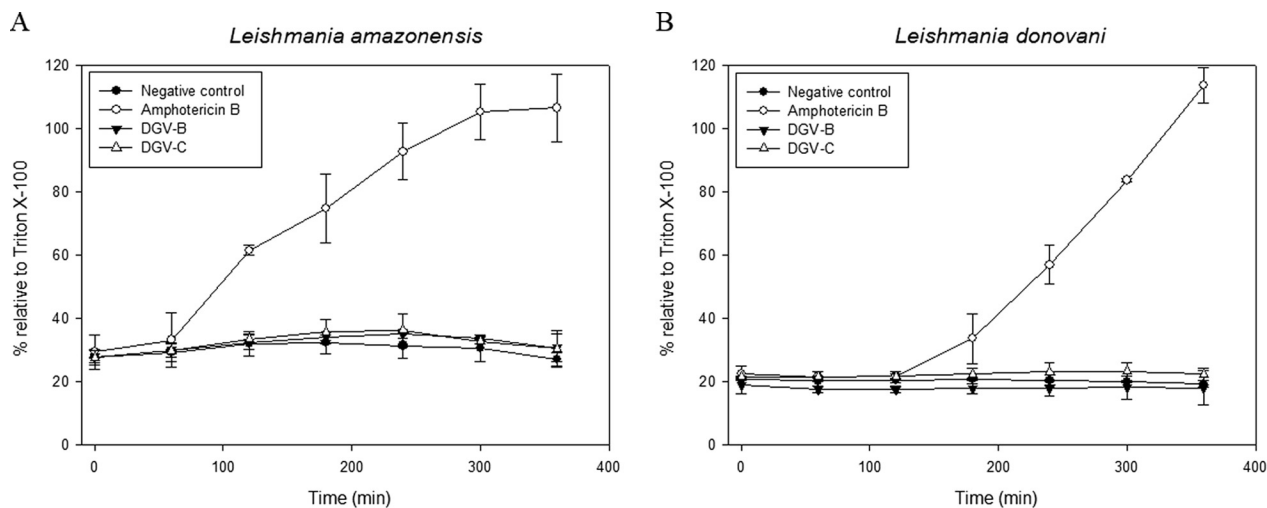


FIG 4 Plasma membrane permeability assay results. (A) *L. amazonensis*. (B) *L. donovani*. Error bars represent the standard deviations (SD). Each data point indicates the mean of the results of three measurements.

and DGV-C molecules. However, results were negative in the case of *L. amazonensis* treated with both molecules (Fig. 5).

Finally, the double-staining results were obtained after 24 h of incubation with the molecules at the IC_{90} and the two fluorescent dyes (Hoechst 33342/propidium iodide). Figure 6 shows the images obtained when the assays were performed. It is clear that the cells treated with DGV-B and DGV-C exhibited chromatin condensation (blue) in the case of *L. amazonensis* and at the same time that the negative control exhibited a soft uniform blue (Fig. 6). Meanwhile, *L. donovani* parasites treated with either of the two HATNs showed strong chromatin condensation (intense blue).

Conclusions. To the best of our knowledge, this is the first time that hexaazatriphthalenes and related compounds have been evaluated as possible novel drugs against any pathogen. All derivatives showed good activity against promastigotes of the two *Leishmania* strains, highlighting the activity of DGV-C. When the HATNs were tested against the intracellular parasites of *L. amazonensis*, only DGV-B and DGV-C maintained the activity, even decreasing the IC_{50} for the amastigote stage.

Certainly, the more cytotoxic molecules corresponded to the more active ones, but we have to emphasize that DGV-C evaluated against intracellular amastigotes presented an IC_{50} 10 times smaller than the CC_{50} , and this difference was more pronounced with DGV-B, with an IC_{50} almost 100 times lower than the CC_{50} , as is reflected in the selectivity index. The dissimilarities between the CC_{50} values of the two molecules might be a consequence of the differences between their molecular weights, since DGV-B is a smaller molecule (284 g/mol) than DGV-C (755 g/mol).

A preclinical study of the toxicity, metabolism, and pharmacokinetic properties of DGV-B, which did not cause any mortality or statistically significant differences in body weights when the drug was administered at 30 mg/kg of body weight intraperitoneally (i.p.) during a 28-day study or at 100 mg/kg orally (p.o.) during a 7-day study, has been published recently. There were no chemical, hematological, or histopathological clinical changes in different organs of mice at those two dosages (30).

Several of the markers typical of mammalian apoptosis have been shown in *Leishmania* spp, which suggested the occurrence of

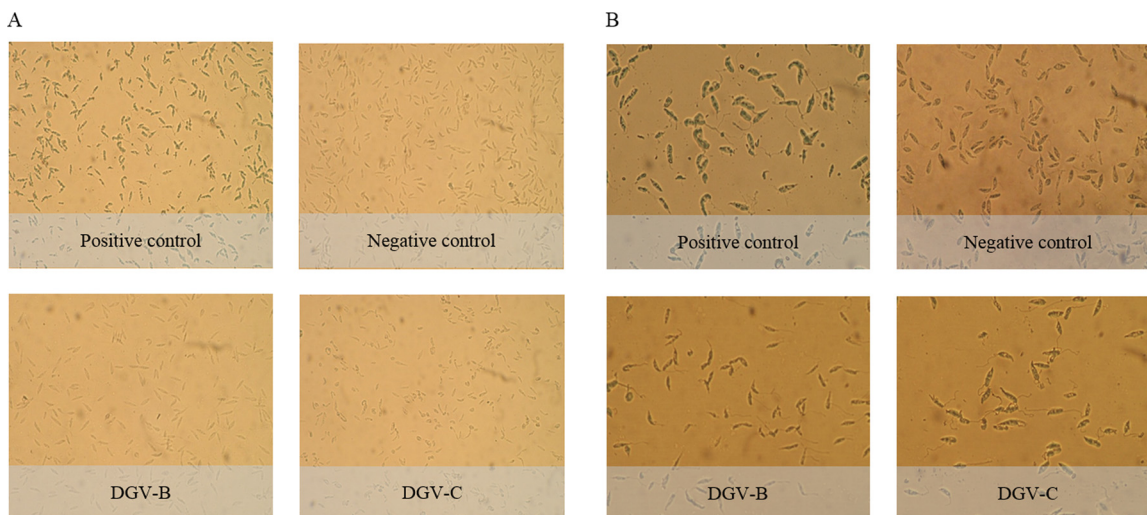


FIG 5 TUNEL assay results. (A) *L. amazonensis*. (B) *L. donovani*.

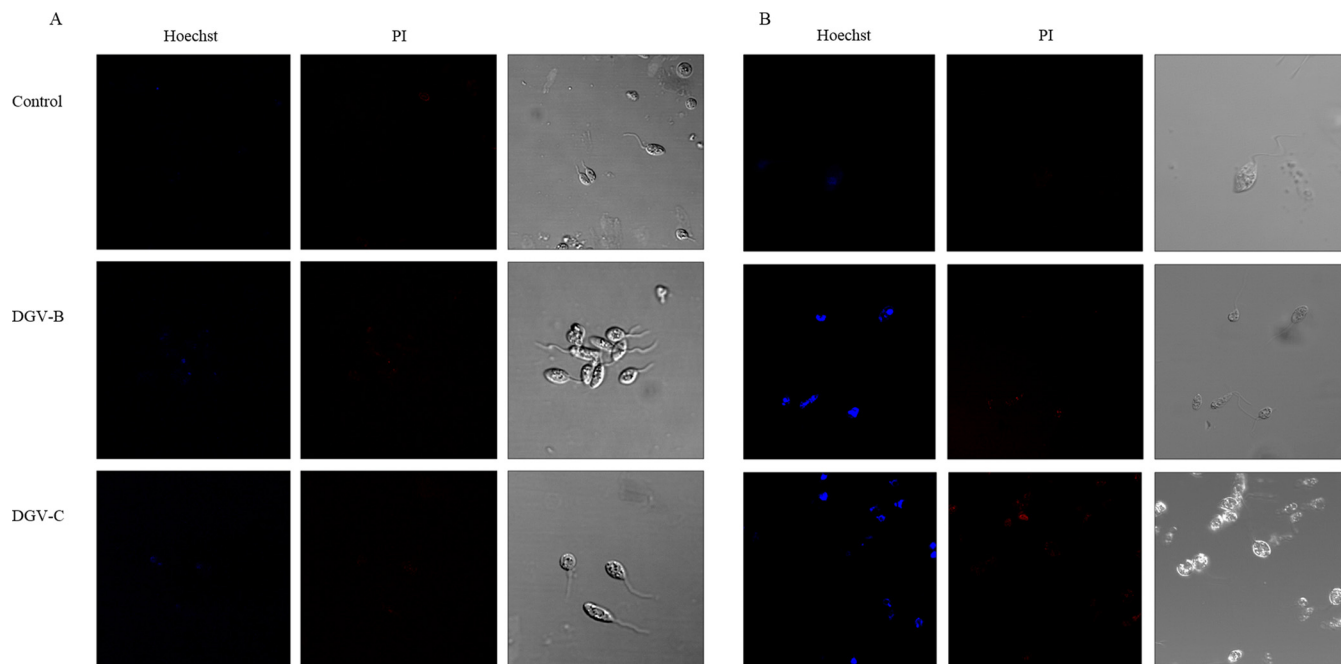


FIG 6 Hoechst-propidium iodide staining results after 24 h of incubation with the IC₅₀ of DGV-B and DGV-C. (A) *L. amazonensis*. (B) *L. donovani*.

apoptosis-like death in these organisms. The biochemical evidence of programmed cell death in *Leishmania* spp. includes the following results: cell shrinkage, nuclear chromatin condensation, DNA fragmentation, membrane blebbing, mitochondrial transmembrane potential loss, cytochrome *c* release, generation of apoptotic bodies, and phosphatidylserine exposure (31). To elucidate the type of parasite death that our molecules were producing, we studied some of these processes.

The apoptosis-like process in *Leishmania* spp. requires ATP to carry out all the involved procedures; therefore, the total loss of mitochondrial potential in an unicellular organism with just one mitochondrion would cause a strong decrease of the survival mechanism, leading the cell to necrosis. Nevertheless, only the mitochondrion of *L. donovani* is able to adopt different states of energy generation in order to maintain ATP levels and parasite viability until the conclusion of the apoptosis-like process. ATP levels have been reported to stay at around 20% after treatment of the parasites with H₂O₂, proving that a minimal level of ATP is maintained to allow the apoptosis-like process of the cell (32).

Moreover, the differences between the two strains of *Leishmania* in the amounts of annexin V observed (higher in *L. amazonensis*) could be due to the differences in the amount of PS present in the membrane of the parasites. While PS represents 32% of the total phospholipids in the membrane in *L. amazonensis* (33), PS represents just 10% of the phospholipids in the cytoplasmic membrane in *L. donovani* (34).

The study of the plasma membrane permeability provides us important data to distinguish between apoptosis and necrosis, considering the rupture of the plasma membrane a morphological feature of the necrosis (35), so in this respect, all of our treatments caused the disruption of the plasma membrane, discarding necrosis processes. Also, the results of this assay could indicate that the target of these molecules is not directly related to the plasma membrane of the parasites (36).

TUNEL-obtained results should be confirmed with additional experiments, since this technique has many critical steps (fixation, permeabilization, etc.) that can produce false-negative as well as false-positive results, and it is possible that this is the case of the results with *L. amazonensis*. Besides, it is possible that, in other parasitic protozoa such as *Plasmodium falciparum*, degraded DNA fragments could be longer and that this degradation could be undetectable using the TUNEL assay and even agarose gel electrophoresis (37).

Taking the results together, DGV-B and DGV-C molecules produce an apoptosis-like process with *L. amazonensis* and *L. donovani* at a very low dose, avoiding an unnecessary immune response; thus, we consider DGV-B and DGV-C to be good compounds for further studies *in vivo*.

ACKNOWLEDGMENTS

This work was supported by grants from RICET (project no. RD12/0018/0012 of the program of Redes Temáticas de Investigación Cooperativa, FIS), Spanish Ministry of Health, Madrid, Spain, and grant PI13/00490 “Protozoosis Emergentes por Amebas de Vida Libre: Aislamiento, Caracterización, Nuevas Aproximaciones Terapéuticas y Traslación Clínica de los Resultados” from the Instituto de Salud Carlos III. A.L.-A. was funded by a grant (“Ayudas del Programa de Formación de Personal Investigador, para la realización de Tesis Doctorales”) from the Agencia Canaria de Investigación, Innovación y Sociedad de la Información, of the Canary Islands government. C.M.-N. was supported by the Canary Islands CIE: Tricontinental Atlantic Campus. M.R.-B. and A.L.-A. were funded by Becas de Investigación Obra Social La Caixa-Fundación CajaCanarias para Posgraduados de la Universidad de La Laguna, Convocatoria 2014. J.L.-M. was supported by the Ramón y Cajal Subprogramme of the Spanish Ministry of Science and Innovation RYC-2011-08863. I.S. was supported by a grant from the Laboratoire Matériaux—Molécules et Applications, IPEST, and Ayudas para estancias estudiantes de posgrado e investigadores del continente americano y africano 2014 from the ULL. The authors are grateful for funds provided to ULL by the Canarian Agency for Research, Innovation and Information Society, 85% cofunded by the European Social Funds.

REFERENCES

- Reithinger R, Dujardin JC, Louzir H, Pirmez C, Alexander B, Brooker S. 2007. Cutaneous leishmaniasis. *Lancet Infect Dis* 7:581–596. [http://dx.doi.org/10.1016/S1473-3099\(07\)70209-8](http://dx.doi.org/10.1016/S1473-3099(07)70209-8).
- Boelaert M, Criel B, Leeuwenburg J, Van Damme W, Le Ray D, Van der Stuyf P. 2000. Visceral leishmaniasis control: a public health perspective. *Trans R Soc Trop Med Hyg* 94:465–471. [http://dx.doi.org/10.1016/S0035-9203\(00\)90055-5](http://dx.doi.org/10.1016/S0035-9203(00)90055-5).
- Hepburn NC. 2000. Cutaneous leishmaniasis. *Clin Exp Dermatol* 25:363–370. <http://dx.doi.org/10.1046/j.1365-2230.2000.00664.x>.
- World Health Organization. 2009. Visceral leishmaniasis therapy: statement on the outcome of a meeting. WHO, Geneva, Switzerland. http://www.who.int/leishmaniasis/resources/Leish_VL_Therapy_statement.pdf. Accessed 2 July 2012.
- Desjeux P. 2004. Leishmaniasis: current situation and new perspectives. *Comp Immunol Microbiol Infect Dis* 27:305–318. <http://dx.doi.org/10.1016/j.cimid.2004.03.004>.
- World Health Organization. 2012. Leishmaniasis: background information. WHO, Geneva, Switzerland. <http://www.who.int/leishmaniasis/en/>.
- Alvar J, Croft S, Olliaro P. 2006. Chemotherapy in the treatment and control of leishmaniasis. *Adv Parasitol* 61:223–274. [http://dx.doi.org/10.1016/S0065-308X\(05\)61006-8](http://dx.doi.org/10.1016/S0065-308X(05)61006-8).
- Olliaro PL. 2010. Drug combinations for visceral leishmaniasis. *Curr Opin Infect Dis* 23:595–602. <http://dx.doi.org/10.1097/QCO.0b013e32833fca9d>.
- Seifert K, Croft SL. 2006. *In vitro* and *in vivo* interactions between miltefosine and other antileishmanial drugs. *Antimicrob Agents Chemother* 50:73–79. <http://dx.doi.org/10.1128/AAC.50.1.73-79.2006>.
- Sundar S, Sinha PK, Rai M, Verma DK, Nawin K, Alam S, Chakravarty J, Vaillant M, Verma N, Pandey K, Kumari P, Lal CS, Arora R, Sharma B, Ellis S, Strub-Wourgaft N, Balasegaram M, Olliaro P, Das P, Modabber F. 2011. Comparison of short-course multidrug treatment with standard therapy for visceral leishmaniasis in India: an open-label, non-inferiority, randomised controlled trial. *Lancet* 377:477–486. [http://dx.doi.org/10.1016/S0140-6736\(10\)62050-8](http://dx.doi.org/10.1016/S0140-6736(10)62050-8).
- Croft SL, Sundar S, Fairlamb AH. 2006. Drug resistance in leishmaniasis. *Clin Microbiol Rev* 19:111–126. <http://dx.doi.org/10.1128/CMR.19.1.111-126.2006>.
- Maltezou HC. 2010. Drug resistance in visceral leishmaniasis. *J Biomed Biotechnol* 2010:617521. <http://dx.doi.org/10.1155/2010/617521>.
- Singh B, Sundar S. 2012. Leishmaniasis: vaccine candidates and perspectives. *Vaccine* 30:3834–3842. <http://dx.doi.org/10.1016/j.vaccine.2012.03.068>.
- Crispin X, Cornil J, Friedlein R, Okudaira KK, Lemaure V, Crispin A, Kestemont G, Lehmann M, Fahlman M, Lazzaroni R, Geerts Y, Wendin G, Ueno N, Bredas JL, Salanek WR. 2004. Electronic delocalization in discotic liquid crystals: a joint experimental and theoretical study. *J Am Chem Soc* 126:11889–11896. <http://dx.doi.org/10.1021/ja048669j>.
- Ishi-i T, Yaguna K, Kuwahara R, Taguri Y, Mataka S. 2006. Self-assembly of n-type semiconductor tri(phenoanthroline) hexaazatri-naphthylene with a large aromatic core. *Org Lett* 8:585–588. <http://dx.doi.org/10.1021/ol052779t>.
- García Velázquez D, González Orive A, Hernández Creus A, Luque R, Gutiérrez Ravelo A. 2011. Novel organogelators based on amine-derived hexaazatri-naphthylene. *Org Biomol Chem* 9:6524–6527. <http://dx.doi.org/10.1039/c1ob05811h>.
- Golubovskaya V, Nyberg C, Zheng M, Kweh F, Magis A, Ostrov D, Cance WC. 2008. A small molecule inhibitor, 1,2,4,5-benzenetetraamine tetrahydrochloride, targeting the γ 397 site of focal adhesion kinase decreases tumor growth. *J Med Chem* 51:7405–7416. <http://dx.doi.org/10.1021/jm800483v>.
- Zheng D, Golubovskaya V, Kurenova E, Wood C, Massoll NA, Ostrov D, Cance WG, Hochwald SN. 2010. A novel strategy to inhibit FAK and IGF-1R decreases growth of pancreatic cancer xenografts. *Mol Carcinog* 49:200–209. <http://dx.doi.org/10.1002/mc.20590>.
- Beierle EA, Ma X, Stewart J, Nyberg C, Trujillo A, Cance WG, Golubovskaya VM. 2010. Inhibition of focal adhesion kinase decreases tumor growth in human neuroblastoma. *Cell Cycle* 9:1005–1015. <http://dx.doi.org/10.4161/cc.9.5.10936>.
- Hochwald SN, Nyberg C, Zheng M, Zheng D, Wood C, Massoll NA, Magis A, Ostrov D, Cance WG, Golubovskaya VM. 2009. A novel small molecule inhibitor of FAK decreases growth of human pancreatic cancer. *Cell Cycle* 8:2435–2443. <http://dx.doi.org/10.4161/cc.8.15.9145>.
- Heffler M, Golubovskaya VM, Dunn KM, Cance W. 2013. Focal adhesion kinase autophosphorylation inhibition decreases colon cancer cell growth and enhances the efficacy of chemotherapy. *Cancer Biol Ther* 14:761–772. <http://dx.doi.org/10.4161/cbt.25185>.
- O'Brien S, Golubovskaya VM, Conroy J, Liu S, Wang D, Liu B, Cance WG. 2014. FAK inhibition with small molecule inhibitor Y15 decreases viability, clonogenicity, and cell attachment in thyroid cancer cell lines and synergizes with targeted therapeutics. *Oncotarget* 5:7945–7959.
- Velázquez DG. 2010. Síntesis y propiedades de entidades moleculares: autoensamblaje mediante fuerzas no covalentes. PhD thesis. University of La Laguna. Tenerife, Canary Islands, Spain.
- Cabrera-Serra MG, Lorenzo-Morales J, Romero M, Valladares B, Piñero JE. 2007. *In vitro* activity of perfosine: a novel alkylphospholipid against the promastigote stage of *Leishmania* species. *Parasitol Res* 100:1155–1157. <http://dx.doi.org/10.1007/s00436-006-0408-4>.
- Jain SK, Sahu R, Walker LA, Tekwani BL. 2012. A parasite rescue and transformation assay for antileishmanial screening against intracellular *Leishmania donovani* amastigotes in THP1 human acute monocytic leukemia cell line. *J Vis Exp* 30:4054. <http://dx.doi.org/10.3791/4054>.
- Lorenzo-Morales J, Martín-Navarro CM, López-Arencibia A, Santana-Morales MA, Afonso-Lehmann RN, Maciver SK, Valladares B, Martínez-Carretero E. 2010. Therapeutic potential of a combination of two gene-specific small interfering RNAs against clinical strains of *Acanthamoeba*. *Antimicrob Agents Chemother* 54:5151–5155. <http://dx.doi.org/10.1128/AAC.00329-10>.
- Sifaoui I, López-Arencibia A, Martín-Navarro CM, Ticona JC, Reyes-Battle M, Mejri M, Jiménez AI, Lopez-Bazzocchi I, Valladares B, Lorenzo-Morales J, Abderabba M, Piñero JE. 2014. *In vitro* effects of triterpenic acids from olive leaf extracts on the mitochondrial membrane potential of promastigote stage of *Leishmania* spp. *Phytomedicine* 21:1689–1694. <http://dx.doi.org/10.1016/j.phymed.2014.08.004>.
- Luque-Ortega JR, Rivas L. 2010. Characterization of the leishmanicidal activity of antimicrobial peptides. *Methods Mol Biol* 618:393–420. http://dx.doi.org/10.1007/978-1-60761-594-1_25.
- Likhitwitayawuid K, Angerhofer CK, Chai H, Pezzuto JM, Cordell GA, Ruangrungsi N. 1993. Cytotoxic and antimalarial alkaloids from the tubers of *Stephania pierrei*. *J Nat Prod* 56:1468–1478. <http://dx.doi.org/10.1021/np50099a005>.
- Golubovskaya V, Curtin L, Groman A, Sexton S, Cance WG. 12 June 2014, posting date. *In vivo* toxicity, metabolism and pharmacokinetic properties of FAK inhibitor 14 or Y15 (1,2,4,5-benzenetetraamine tetrahydrochloride). *Arch Toxicol* <http://dx.doi.org/10.1007/s00204-014-1290-y>.
- Bruchhaus I, Roeder T, Renneberg A, Heussler VT. 2007. Protozoan parasites: programmed cell death as a mechanism of parasitism. *Trends Parasitol* 23:376–383. <http://dx.doi.org/10.1016/j.pt.2007.06.004>.
- Mukherjee SB, Das M, Sudhandiran G, Shaha C. 2002. Increase in cytosolic Ca²⁺ levels through the activation of non-selective cation channels induced by oxidative stress causes mitochondrial depolarization leading to apoptosis-like death in *Leishmania donovani* promastigotes. *J Biol Chem* 277:24717–24727. <http://dx.doi.org/10.1074/jbc.M201961200>.
- Rodríguez JC, Attias M, Rodríguez C, Urbina JA, de Souza W. 2002. Ultrastructural and biochemical alterations induced by 22,26-azasterol, a delta(24(25))-sterol methyltransferase inhibitor, on promastigote and amastigote forms of *Leishmania amazonensis*. *Antimicrob Agents Chemother* 46:487–499. <http://dx.doi.org/10.1128/AAC.46.2.487-499.2002>.
- Wassef MK, Fioretti TB, Dwyer DM. 1985. Lipid analyses of isolated surface membranes of *Leishmania donovani* promastigotes. *Lipids* 20:108–115. <http://dx.doi.org/10.1007/BF02534216>.
- Kroemer G, Galluzzi L, Vandenabeele P, Abrams J, Alnemri ES, Baehrecke EH, Blagosklonny MV, El-Deiry WS, Golstein P, Green DR, Hengartner M, Knight RA, Kumar S, Lipton SA, Malorni W, Núñez G, Peter ME, Tschopp J, Yuan J, Piacentini M, Zhivotovskiy B, Melino G, Nomenclature Committee on Cell Death 2009. 2009. Classification of cell death: recommendations of the Nomenclature Committee on Cell Death 2009. *Cell Death Differ* 16:3–11. <http://dx.doi.org/10.1038/cdd.2008.150>.
- Bou DD, Tempone AG, Pinto É Lago GJH, Sartorelli P. 2014. Antiparasitic activity and effect of casearins isolated from *Casearia sylvestris* on *Leishmania* and *Trypanosoma cruzi* plasma membrane. *Phytomedicine* 21:676–681. <http://dx.doi.org/10.1016/j.phymed.2014.01.004>.
- Nyakeriga AM, Perlmann H, Hagstedt M, Berzins K, Troye-Blomberg M, Zhivotovskiy B, Perlmann P, Grandien A. 2006. Drug-induced death of the asexual blood stages of *Plasmodium falciparum* occurs without typical signs of apoptosis. *Microbes Infect* 8:1560–1568. <http://dx.doi.org/10.1016/j.micinf.2006.01.016>.